

We are IntechOpen, the world's leading publisher of Open Access books Built by scientists, for scientists

6,900

Open access books available

185,000

International authors and editors

200M

Downloads

Our authors are among the

154

Countries delivered to

TOP 1%

most cited scientists

12.2%

Contributors from top 500 universities



WEB OF SCIENCE™

Selection of our books indexed in the Book Citation Index
in Web of Science™ Core Collection (BKCI)

Interested in publishing with us?
Contact book.department@intechopen.com

Numbers displayed above are based on latest data collected.
For more information visit www.intechopen.com



Electric Components of Acoustic Waves in the Vicinity of Nonpiezoactive Directions

V.I. Alshits, V.N. Lyubimov and A. Radowicz

Additional information is available at the end of the chapter

<http://dx.doi.org/10.5772/56067>

1. Introduction

The acoustic wave of displacements in piezoelectric media is usually accompanied by a quasistatic wave of the electric potential. This implies that, using acoustic waves, electric signals can be transmitted over a crystal at the velocity of sound. Such possibility opened the way to numerous applications of acoustic waves in electronic devices and even led to the formation of a special field of science called acoustoelectronics. The applied aspect provides an important stimulus for extensive investigations devoted to various features of acoustic fields in piezoelectric crystals (Royer & Dieulesaint, 2000). These investigations are also stimulated by basic interest in the study of new effects in media with electromechanical couplings (Lyubimov, 1968; Balakirev & Gilinskii, 1982; Lyamov, 1983). The acoustics of piezoelectric crystals is still an extensively developing field of solid state physics [see, e.g., the review article by Gulyaev (1998)], the more so that even purely basic investigations in this field frequently contain ideas for fruitful, however not immediately evident, applications.

It should also be noted that the anisotropy often influences the properties of piezoelectric crystals in a nontrivial way, and may sometimes lead to qualitatively new phenomena. In particular, it is very important from the practical standpoint to know the wave propagation directions \mathbf{m} for which the electric field components possess maximum amplitudes (Alshits & Lyubimov, 1990) and, on the contrary, to reveal the nonpiezoactive directions (Royer & Dieulesaint, 2000; Lyamov, 1983) in which the electric signals are not transmitted. Taking into account that, irrespective of the anisotropy, the electric field in an acoustic wave is always longitudinal ($\mathbf{E} \parallel \mathbf{m}$) and the electric induction is always transverse ($\mathbf{D} \perp \mathbf{m}$), we have to distinguish (Lyamov, 1983) between the directions of longitudinal and transverse nonpiezoactivity in which $\mathbf{E} = 0$ and $\mathbf{D} = 0$, respectively. This paper presents the results of investigations aimed at a detailed analysis of the nonpiezoactivity of both types.

Another important aspect of this problem is related to directions \mathbf{m} , in the vicinity of which the vector fields of displacements (\mathbf{u}) and the accompanying electric components (\mathbf{E} , \mathbf{D}) exhibit singularities. According to the results obtained by Alshits, Sarychev & Shuvalov (1985), Alshits *et al* (1987), and Shuvalov (1998) this very situation takes place near the acoustic axes, where the orientational singularities in the degenerate branches of eigenwaves are observed for the \mathbf{u} and \mathbf{D} fields, and the amplitude singularities, for the \mathbf{E} field. This paper deals with orientational singularities of another type, which occur in the vicinity of the transverse nonpiezoactivity directions in the vector fields $\mathbf{D}(\mathbf{m})$, i.e. around the points \mathbf{m}_0 on the unit sphere such that $\mathbf{D}(\mathbf{m}_0) = 0$ (Alshits, Lyubimov & Radowicz, 2005 a, b).

Below we will formulate the equations determining special directions \mathbf{m} for which either $\mathbf{E}_a(\mathbf{m}) = 0$ or $\mathbf{D}_a(\mathbf{m}) = 0$ for all three branches of the acoustic spectrum ($a = 1, 2, 3$). These directions have different dimensionalities: the typical solutions appear as lines of zero electric field ($\mathbf{E}_a = 0$) and points of zero induction ($\mathbf{D}_a = 0$) on the unit sphere $\mathbf{m}^2 = 1$. The equations obtained will be analyzed both in the general case and in application to various particular crystal symmetry classes. The two types on nonpiezoactivity are closely related to the crystal symmetry, but they can also exist in triclinic crystals possessing no elements of symmetry. The corresponding theorems of existence are proved.

The possible types of singularities in the vector field $\mathbf{D}_a(\mathbf{m})$ in the vicinity of the transverse nonpiezoactivity directions will be considered. In particular, it will be shown that, depending on the material moduli, the singularity in an isolated point \mathbf{m}_0 may be characterized by the Poincaré indices (topological charges) $n_D = 0, \pm 1, \pm 2$. The general analytical expressions will be obtained for the n_D values in triclinic crystals with arbitrary anisotropy and specified for a large series of crystals belonging to particular crystal symmetry classes. Only the solutions corresponding to singularities with $n_D = \pm 1$ are topologically stable, while singularities of the other types either split or disappear upon an arbitrary triclinic perturbation of the material tensors. However, the sum of indices for any splitting must be equal to the initial index n_D .

The chapter is mainly based on our papers (Alshits, Lyubimov & Radowicz, 2005 a, b).

2. Statement of the problem and general equations

In piezoelectric crystals, purely mechanical characteristics, the elastic displacement vector $\mathbf{u}(\mathbf{r}, t)$, the distortion tensor $\hat{\beta}(\mathbf{r}, t)$, and the stress tensor $\hat{\sigma}(\mathbf{r}, t)$, are related to such electrical quantities as the potential $\phi(\mathbf{r}, t)$ and the electric field strength $\mathbf{E}(\mathbf{r}, t)$, and induction $\mathbf{D}(\mathbf{r}, t)$. The fields of $\hat{\beta}(\mathbf{r}, t)$ and $\mathbf{E}(\mathbf{r}, t)$ can be expressed in terms of their own potentials as

$$\hat{\beta}(\mathbf{r}, t) = \nabla \mathbf{u}(\mathbf{r}, t), \quad \mathbf{E}(\mathbf{r}, t) = -\nabla \phi(\mathbf{r}, t). \quad (1)$$

The interrelation of these characteristics is determined by the constitutive equations (Landau & Lifshitz, 1984):

$$\sigma_{ij} = c_{ijkl}\beta_{kl} - e_{kij}E_k, \quad D_i = e_{ikl}\beta_{kl} + \varepsilon_{ik}E_k, \quad (2)$$

where $c_{ijkl} = \hat{c}$ is the tensor of elastic moduli, $e_{kij} = \hat{e}$ is the tensor of piezoelectric moduli, and $\varepsilon_{ik} = \hat{\varepsilon}$ is the permittivity tensor. In such a piezoelectric medium, the bulk acoustic wave with the phase velocity v and the wave vector $\mathbf{k} = k\mathbf{m}$ must be a superposition of mechanical and electrical dynamic fields:

$$\{\mathbf{u}, \varphi\} = \{\mathbf{u}_0, \varphi_0\} \exp\{ik(\mathbf{m} \cdot \mathbf{r} - vt)\}. \quad (3)$$

These fields obey the usual equations of motion (Landau & Lifshitz, 1984):

$$\text{Div } \hat{\sigma} = \rho \ddot{\mathbf{u}}, \quad \text{Div } \mathbf{D} = 0, \quad (4)$$

where ρ is the density of medium. Here, we use the well-known quasi-static approximation valid to within the terms proportional to the ratio $(v/c)^2 \sim 10^{-10}$ (c is the velocity of light). Combining the above relations, we readily obtain a homogeneous equation for the polarization vector \mathbf{u}_0 (Landau & Lifshitz, 1984):

$$\hat{F}(v, \mathbf{m})\mathbf{u}_0 \equiv [\hat{F}^{(0)} + \mathbf{e} \otimes \mathbf{e} / \varepsilon]\mathbf{u}_0 = 0, \quad (5)$$

where

$$\hat{F}^{(0)} = \mathbf{mcm} - \rho v^2 \hat{I}, \quad \mathbf{e} = \mathbf{m}\hat{e}\mathbf{m}, \quad \varepsilon = \mathbf{m} \cdot \hat{\varepsilon} \mathbf{m}, \quad (6)$$

symbol \otimes denotes the dyadic product, and \hat{I} is the unit matrix. A necessary condition for the existence of nontrivial solutions of the homogeneous equation (5) is

$$\det \hat{F}(v, \mathbf{m}) = 0. \quad (7)$$

This is a cubic equation for the square of phase velocity v , which determines the three branches of the velocity of the bulk acoustic waves $v_\alpha(\mathbf{m})$ ($\alpha = 1, 2, 3$).

Orientations of the corresponding mutually orthogonal polarization vectors $\mathbf{u}_{0\alpha}(\mathbf{m})$ of the isonormal eigenwaves can be expressed in terms of the \hat{F}_α matrix, which is adjoint to the matrix $\hat{F}_\alpha(\mathbf{m}) \equiv \hat{F}_\alpha(v_\alpha(\mathbf{m}), \mathbf{m})$ and is determined from the condition $\overline{\hat{F}_\alpha} \hat{F}_\alpha = \hat{I} \det \hat{F}_\alpha$. As can be readily checked, Eq. (5) for any vector \mathbf{c} such that $\overline{\hat{F}_\alpha} \mathbf{c} \neq 0$ is satisfied for

$$\mathbf{u}_{0\alpha}(\mathbf{m}) \parallel \overline{\hat{F}_\alpha}(\mathbf{m})\mathbf{c}. \quad (8)$$

It should be emphasized that the direct relation (8) between the polarization vector $\mathbf{u}_{0\alpha}(\mathbf{m})$ and the wave normal \mathbf{m} will be widely used in the subsequent analysis.

Once the field of elastic displacements for a given wave branch $\mathbf{u}_a(\mathbf{r}, t)$ is known, we can also determine the corresponding electric components (Landau & Lifshitz, 1984). For the subsequent analysis, these components are conveniently represented [by analogy with Eqs. (3)–(8)] in a coordinate-free form as

$$\phi_a = \mathbf{e} \cdot \mathbf{u}_a / \varepsilon, \quad \mathbf{E}_a = -ik\phi_a \mathbf{m}, \quad \mathbf{D}_a = ik\hat{N}\mathbf{u}_a, \quad (9)$$

$$\hat{N} = \hat{\mathbf{e}}\mathbf{m} - (\hat{\mathbf{e}}\mathbf{m}) \otimes \mathbf{m} \cdot \hat{\mathbf{e}}\mathbf{m} / \mathbf{m} \cdot \hat{\mathbf{e}}\mathbf{m}. \quad (10)$$

Relations (9) together with condition (8) determine the functions $\mathbf{E}_a(\mathbf{m})$ and $\mathbf{D}_a(\mathbf{m})$ necessary for the subsequent analysis.

As can be readily seen, $\mathbf{m}\hat{N} \equiv 0$. This identity and the third relation in (9) clearly illustrate the well-known property (see Introduction) according to which the electric field $\mathbf{E}_a(\mathbf{m})$ is purely longitudinal, whereas the induction $\mathbf{D}_a(\mathbf{m})$ is purely transverse:

$$\mathbf{E}_a \parallel \mathbf{m}, \quad \mathbf{D}_a \perp \mathbf{m}. \quad (11)$$

On the other hand, the same identity $\mathbf{m}\hat{N} = 0$ implies one useful property of the \hat{N} matrix:

$$\det \hat{N} = 0, \quad (12)$$

which indicates that this matrix is planar and, hence, can be represented as a sum of two dyads.

3. Examples of transversely isotropic piezoelectrics

There are three groups of piezoelectrics which exhibit a transverse isotropy of their acoustic properties. They belong to the following classes of symmetry (Sirotnin & Shaskolskaya, 1982):

$$\infty 2, 622, \quad (13)$$

$$\infty m, 6mm, \quad (14)$$

$$\infty, 6. \quad (15)$$

Owing to the transverse isotropy, the formulas presented below contain only the polar angle θ between the \mathbf{m} vector and the z axis coinciding with the principal axis of symmetry. Without loss of generality, we may proceed with the analysis upon selecting any cross section containing the main axis. Here, it is convenient to choose

$$\mathbf{m} = (m_1, 0, m_3) = (\sin\theta, 0, \cos\theta). \quad (16)$$

In these coordinates, the $\hat{F}^{(0)}$ matrix in Eq. (6) for all the six classes of symmetry (13)–(15) has the same quasi-diagonal form (Fedorov, 1968):

$$\hat{F}^{(0)} = \begin{pmatrix} c_{11}m_1^2 + c_{44}m_3^2 - \rho v^2 & 0 & dm_1m_3 \\ 0 & c_{66}m_1^2 + c_{44}m_3^2 - \rho v^2 & 0 \\ dm_1m_3 & 0 & c_{44}m_1^2 + c_{33}m_3^2 - \rho v^2 \end{pmatrix}, \quad (17)$$

where $d = c_{13} + c_{44}$. The $\hat{\mathbf{e}}\mathbf{m}$ vector and, hence, the ε scalar in Eq. (6) are also the same for all symmetry classes (13)–(15) (Sirotnin & Shaskolskaya, 1982):

$$\hat{\mathbf{e}}\mathbf{m} = (\varepsilon_1 m_1, 0, \varepsilon_3 m_3), \quad \varepsilon = \varepsilon_1 m_1^2 + \varepsilon_3 m_3^2. \quad (18)$$

However, the form of the electric vector \mathbf{e} according to Eq. (6) for the transversely isotropic crystals of three types is different. For the piezoelectric media belonging to classes (13) and (14), the electric vectors are expressed as

$$\mathbf{e} = e_{14}(0, m_1 m_3, 0), \quad (19)$$

$$\mathbf{e} = \{(e_{15} + e_{31})m_1 m_3, 0, e_{15}m_1^2 + e_{33}m_3^2\}, \quad (20)$$

respectively. For a medium of the symmetry class (15), the electric vector is given by a sum of expressions (19) and (20). Thus, the structure of the \hat{F} matrix in (5) for classes (13) and (14) is the same as in (17), but this conclusion is not valid for the \hat{F} matrix of the symmetry classes (15), which contains no vanishing elements. In the same coordinates, the matrix for the piezoelectric media belonging to classes (13) and (14) has the following forms:

$$\hat{N} = e_{14} \begin{pmatrix} 0 & (\varepsilon_3 / \varepsilon)m_3^2 & 0 \\ -m_3 & 0 & -m_1 \\ 0 & -(\varepsilon_3 / \varepsilon)m_1 m_3^2 & 0 \end{pmatrix}, \quad (21)$$

$$\hat{N} = \begin{pmatrix} e_{15}m_3 & 0 & e_{15}m_1 \\ 0 & e_{15}m_3 & 0 \\ e_{31}m_1 & 0 & e_{33}m_3 \end{pmatrix} - \varepsilon^{-1} \begin{pmatrix} (e_{15} + e_{31})\varepsilon_1 m_1^2 m_3 & 0 & (e_{15}m_1^2 + e_{33}m_3^2)\varepsilon_1 m_1 \\ 0 & 0 & 0 \\ (e_{15} + e_{31})\varepsilon_3 m_1 m_3^2 & 0 & (e_{15}m_1^2 + e_{33}m_3^2)\varepsilon_3 m_3 \end{pmatrix}, \quad (22)$$

respectively. For a medium of the symmetry classes (15), the matrix \hat{N} is (by analogy with vector \mathbf{e}) given by a sum of expressions (21) and (22). In classes (13) and (14) of higher symmetry, one of the eigenwave branches for any direction \mathbf{m} is purely transverse:

$$\mathbf{u}_t \parallel (0, 1, 0), \quad \rho v_t^2 = c_{66}m_1^2 + c_{44}m_3^2 + (e_{14}^2 / \varepsilon)m_1^2 m_3^2. \quad (23)$$

Such purely transverse waves of the t mode polarized orthogonally to the propagation plane are frequently called SH waves. The other two branches are polarized in the $\{m_1, m_3\}$ plane:

$$\begin{aligned} \mathbf{u}_{l,t'} \parallel (2dm_1m_3, 0, -\Delta_{14}^-m_1^2 + \Delta_{34}^-m_3^2 \pm R), \\ \rho v_{l,t'}^2 = (\Delta_{14}^+m_1^2 + \Delta_{34}^+m_3^2 \pm R) / 2, \end{aligned} \quad (24)$$

where

$$\begin{aligned} R = \sqrt{(\Delta_{14}^-m_1^2 - \Delta_{34}^-m_3^2)^2 + (2dm_1m_3)^2}, \\ \Delta_{ij}^\pm = c_{ii} \pm c_{jj}. \end{aligned} \quad (25)$$

The electric components of the above wave fields can be also determined for an arbitrary direction \mathbf{m} . For a medium of the symmetry class (13):

$$\begin{aligned} \phi_t &= (e_{14} / \varepsilon) m_1 m_3 u_t, \\ \mathbf{D}_t &\parallel e_{14} (\varepsilon_3 / \varepsilon) m_3^2 (m_3, 0, -m_1) u_t, \\ \phi_{l,t'}(\mathbf{m}) &\equiv 0, \\ \mathbf{D}_{l,t'} &\parallel -e_{14} (0, 1, 0) [m_1(\mathbf{u}_{l,t'})_3 + m_3(\mathbf{u}_{l,t'})_1]. \end{aligned} \quad (26)$$

For the less simple symmetry class (14), we present only the result for the SH-branch (23):

$$\phi_t(\mathbf{m}) \equiv 0, \quad \mathbf{D}_t \parallel (0, e_{15} m_3, 0) u_t. \quad (27)$$

The structure of acoustic waves in media of the symmetry classes (15) is more complicated. In this case, even a purely transverse solution ($\mathbf{u}_t \parallel y$) exists only in the xy basis plane.

4. Lines of zero electric field on the unit sphere

According to the second relation in (9), the electric field amplitude distribution on the unit sphere of the wave propagation directions is described by the equation

$$\mathbf{E}_a(\mathbf{m}) = \text{const} \cdot \phi_a(\mathbf{m}) \mathbf{m}, \quad (28)$$

which shows that zero values of $\mathbf{E}_a(\mathbf{m})$ coincide with those of the potential $\phi_a = \mathbf{e} \cdot \mathbf{u}_a / \varepsilon$. According to condition (8), these directions are determined by the equation,

$$\mathbf{e}(\mathbf{m}) \cdot \hat{\bar{F}}_a(\mathbf{m}) \mathbf{c} = 0. \quad (29)$$

The acoustic waves (3) propagating in these directions contain no electrostatic components \mathbf{E}_a , as in a nonpiezoelectric medium. Even a nonzero induction field $D_i = e_{ijk} u_{k,j}$ in these directions does not influence the parameters of the displacement wave.

The scalar equation (29) poses only one limitation on the direction of the wave normal $\mathbf{m} \equiv \mathbf{m}(\theta, \varphi)$ as a function of two spherical angular coordinates. In other words, Eq. (29) determines a line (or several lines) of nonpiezoelectric directions (in which $\mathbf{E}_a = 0$) on the sphere $\mathbf{m}^2 = 1$. It should be noted that the condition of longitudinal nonpiezoactivity,

$$\mathbf{e}(\mathbf{m}) \perp \mathbf{u}_a(\mathbf{m}), \quad (30)$$

in some special cases can be satisfied even on the whole $\mathbf{m}^2 = 1$ sphere. This takes place, in particular, in the transversely isotropic crystals belonging to the symmetry classes (13) (for the l and t' modes (26)) and (14) (for the t mode (27)). For all other crystals, including transversely isotropic crystals belonging to the symmetry classes (15), the geometric locus of the longitudinal nonpiezoactivity has the form of lines on the unit sphere $\mathbf{m}^2 = 1$. Such lines also exist in the piezoactive branches of the aforementioned high-symmetry media belonging to symmetry classes (13) and (14). For example, the zero-field lines $\mathbf{E}_a = 0$ in the l and t' branches of the media of classes (14) and (15) appear at the intersection of the $\mathbf{m}^2 = 1$ sphere with the cones of directions defined by the polar angles θ_l and $\theta_{t'}$ as

$$\tan^2 \theta_l = -e_{33} / (2e_{15} + e_{31}), \quad \tan^2 \theta_{t'} = (e_{15} + e_{31} - e_{33}) / e_{15}. \quad (31)$$

For simplicity, these expressions are written in an approximate form corresponding to the case of a weak electromechanical interaction and a small elastic anisotropy. Nevertheless, one can readily check that the exact condition for the existence of the aforementioned nonpiezoactivity cones is the positive determinacy of the right-hand parts of the approximate formulas (31).

It is possible to prove that the longitudinal nonpiezoactivity lines in fact exist practically in all (even triclinic) crystals. Let us consider a crystal with arbitrary anisotropy, which contains at least one acoustic axis of the general (conical) type. Here, it should be noted that no one real crystal without acoustic axes and no one triclinic crystal without conical axes are known so far. As was demonstrated by Alshits & Lothe (1979) and Holm (1992), the polarization fields of elastic displacements $\mathbf{u}_{0a}(\mathbf{m})$ for the bulk eigenwaves in such a crystal can be arranged on the $\mathbf{m}^2 = 1$ sphere so that one is even,

$$\mathbf{u}_{02}(-\mathbf{m}) = \mathbf{u}_{02}(\mathbf{m}), \quad (32)$$

and two are odd,

$$\mathbf{u}_{01}(-\mathbf{m}) = -\mathbf{u}_{01}(\mathbf{m}), \quad \mathbf{u}_{03}(-\mathbf{m}) = -\mathbf{u}_{03}(\mathbf{m}). \quad (33)$$

The nondegenerate branch $\mathbf{u}_{03}(\mathbf{m})$ is always odd and continuous on the entire sphere of wave directions. As for the degenerate branches, $\mathbf{u}_{01}(\mathbf{m})$ and $\mathbf{u}_{02}(\mathbf{m})$, their evenness depends on the representation and can be changed simultaneously. These branches are continuous at all points of the sphere except for some open-ended lines on which the $\mathbf{u}_{01}(\mathbf{m})$ and $\mathbf{u}_{02}(\mathbf{m})$ functions change sign. Such “anti-sign” lines can be arbitrarily deformed on the unit sphere without changing the positions of end points (coinciding with the points of degeneracy). In fact, the representation is chosen by setting certain fixed positions of the anti-sign lines (coinciding for both degenerate branches).

One can readily check that the aforementioned properties of the fields of elastic displacements, which were established in (Alshits & Lothe, 1979; Holm, 1992) for purely elastic media, are also valid for piezoelectrics. Taking into account that, according to relations (33), the $\mathbf{u}_{03}(\mathbf{m})$ function is odd and the $\mathbf{e}(\mathbf{m})$ function is [by definition (6)] even, we may conclude that the potential

$$\phi_{03}(\mathbf{m}) = \mathbf{e}(\mathbf{m}) \cdot \mathbf{u}_{03}(\mathbf{m}) / \varepsilon$$

is an odd function

$$\phi_{03}(-\mathbf{m}) = -\phi_{03}(\mathbf{m}). \quad (34)$$

This result implies that, for any path connecting the opposite points \mathbf{m} and $-\mathbf{m}$ on the unit sphere, there exists at least one point \mathbf{m}_0 such that $\phi_{03}(\mathbf{m}_0) = 0$. In scanning the paths on the unit sphere, points \mathbf{m}_0 will apparently form a closed line representing a geometric locus of the directions of longitudinal nonpiezoactivity for the nondegenerate branch.

For the degenerate branches $\phi_{01}(\mathbf{m})$ and $\phi_{02}(\mathbf{m})$, the considerations should be somewhat modified, while being still generally analogous to those used in solving a similar problem (Alshits & Lothe, 1979) concerning the existence of the lines of solutions for exceptional bulk waves related to the same degenerate branches in semi-infinite elastic media. Not reproducing these considerations here, we only formulate the result: the longitudinal nonpiezoactivity lines exist in both degenerate branches and pass from one branch to another at the degeneracy points. Thus, the following theorem of existence is valid:

All three wave branches in an arbitrary crystal, which contains conical acoustic axes, must possess lines of longitudinal nonpiezoactivity directions on the unit sphere.

It should be also noted that, when a wave propagates along an acoustic axis \mathbf{m}_d of any type, the continuum of possible orientations of the wave polarization \mathbf{u} in the plane of degeneracy always contains a vector orthogonal to the $\mathbf{e}(\mathbf{m}_d)$ direction. In view of the criterion (30), this ensures nonpiezoactivity of the corresponding wave. Therefore,

acoustic axes must belong to the lines of longitudinal nonpiezoactivity.

The elements of crystal symmetry can become an additional factor accounting for the phenomenon of nonpiezoactivity. According to (Royer & Dieulesaint, 2000), also

symmetry axes determine the directions of longitudinal nonpiezoactivity for purely transverse modes, while

a symmetry plane is the geometric locus of directions of longitudinal nonpiezoactivity for the related SH waves.

One can add that

the planes orthogonal to symmetry axes of even order are the geometric locus of directions of longitudinal nonpiezoactivity for in-plane polarized waves.

Let us consider, for example, a monoclinic piezoelectric crystal belonging to one of the two possible symmetry classes: m or 2 . In the first case, the electric vector \mathbf{e} of any wave propagating in a plane of symmetry m must, obviously, lie in the same plane being, hence, orthogonal to the polarization vector \mathbf{u}_{0t} of all SH waves of the t branch. In the second case, the \mathbf{e} vector for a wave normal occurring in the plane perpendicular to the dyad (2-fold) axis of symmetry must be parallel to this axis and, hence, orthogonal to polarization vectors (belonging to said plane) of the l and t' waves. Naturally, the latter property is valid for any other symmetry axis of even order. In monograph (Royer & Dieulesaint, 2000), this rule was formulated for planes orthogonal to the tetrad (4-fold) and hexad (6-fold) axes.

The above theorems are summarized in Table 1.

| Directions of nonpiezoactivity | Directions of acoustic and symmetry axes | Any direction in symmetry planes | Any direction in planes orthogonal to symmetry axes of even order |
|--------------------------------|--|----------------------------------|---|
| Wave branches | Transverse waves | SH waves | In-plane polarized waves |

Table 1. Directions of obligatory longitudinal nonpiezoactivity ($\mathbf{E}_a = 0$) in crystals

In particular, the coordinate planes of the crystal system orthogonal to the tetrad and dyad axes in cubic piezoelectrics (symmetry classes $\bar{4}3m$ and 23) must be nonpiezoactive for the corresponding l and t' branches. At the same time, the diagonal symmetry planes $\{110\}$ are nonpiezoactive for the corresponding t (SH) waves. One can check that, in the vicinity of the coordinate axes, the potential amplitudes for these branches can be represented in spherical coordinates (θ, φ) as (Fig. 1)

$$\phi_{l,t'} \propto \theta^2 \sin 2\varphi, \quad (35)$$

$$\phi_t \propto \theta^2 \cos 2\varphi. \quad (36)$$

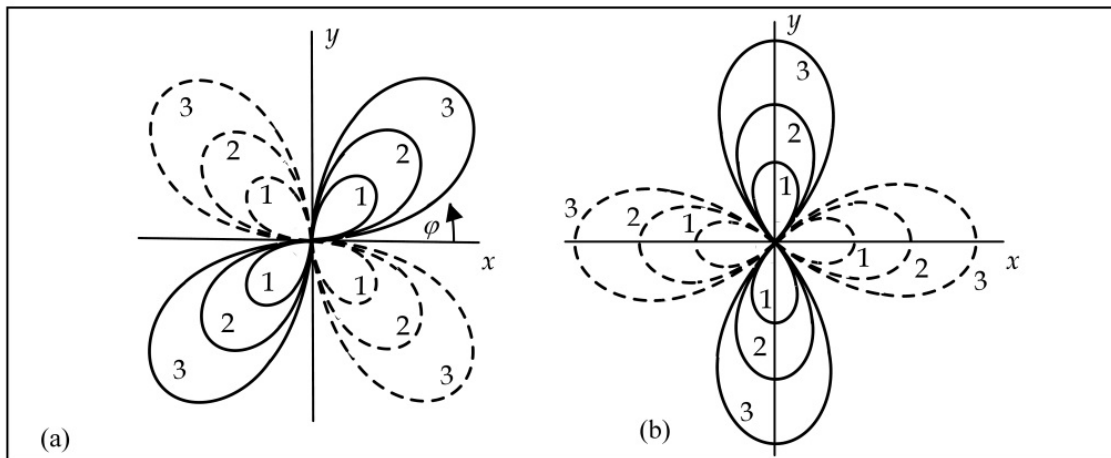


Figure 1. Polar diagrams of the electric potentials (a) $\phi_{l,t'}(\varphi)$ and (b) $\phi_t(\varphi)$ at $\theta = \text{const}$ in the vicinity of the $(0, 0, 1)$ direction in a cubic piezoelectric crystal. Numbers 1, 2, and 3 refer to the angles $\theta_1 < \theta_2 < \theta_3$; solid and dashed lines relate to the potentials of different signs.

5. Zero-induction points on the unit sphere

5.1. General case of arbitrary anisotropy

Now let us consider the conditions determining the propagation directions \mathbf{m}_0 in which the electric induction vector $\mathbf{D}_a = ik\hat{N}\mathbf{u}_a$ defined in (9) vanishes. Taking into account identity (12) and the definition of the adjoint tensor

$$\hat{N}\bar{\hat{N}} = \hat{I}\det\hat{N}, \quad (37)$$

one can readily check that $\mathbf{D}_a = 0$ for the directions \mathbf{m}_0 such that $\mathbf{u}_a \parallel \bar{\hat{N}}\mathbf{d}$, where \mathbf{d} is any vector obeying the condition $\bar{\hat{N}}\mathbf{d} \neq 0$. For these directions \mathbf{m}_0 , according to condition (8), we also have

$$\bar{\hat{F}}_a(\mathbf{m})\mathbf{c} \parallel \bar{\hat{N}}\mathbf{d} \quad (38)$$

In the general case, this condition gives two equations with two unknowns θ and φ , which determine the positions of isolated points $\mathbf{m}_0(\theta, \varphi)$ such that $\mathbf{D}_a = 0$ on the unit sphere $\mathbf{m}^2 = 1$. There is the well-known Brouwer theorem in the topology, according to which

any continuous transform on a sphere, not mapping any point by its antipode, has at least two stationary points.

Now let us consider a distribution of vectors $\mathbf{D}_a(\mathbf{m})$ continuous everywhere on the unit sphere. The continuity of $\mathbf{D}_a(\mathbf{m})$ is ensured when the corresponding branch α is nondegenerate. According to Brouwer's theorem, this distribution of \mathbf{D}_a vectors tangent to the sphere must have two stationary points for which $\mathbf{D}_a = 0$. On the other hand, relations (9) and (10) imply that this distribution also possesses an additional property: $\mathbf{D}_a(-\mathbf{m}) \parallel \mathbf{D}_a(\mathbf{m})$. For this reason, the pair of points stipulated by Brouwer's theorem includes the inversion-equivalent stationary points \mathbf{m}_0 and $-\mathbf{m}_0$. Thus, the following theorem of existence of the transverse nonpiezoactivity directions is valid:

In any crystal of unrestricted anisotropy each nondegenerate branch must contain at least one pair of inversion-equivalent zero-induction points $\pm\mathbf{m}_0$ such that $\mathbf{D}_a(\pm\mathbf{m}_0) = 0$ on the unit sphere.

Therefore, the zero-induction points in a wave field $\mathbf{D}_a(\mathbf{m})$ must exist even in triclinic crystals. Of course, the positions of such points in the general case (i.e., the solutions of Eq. (38) in the general form) cannot be found analytically. However, in some more symmetric crystals, nonpiezoactive directions \mathbf{m}_0 can be found without cumbersome computations.

5.2. Zero-induction points related to elements of the crystal symmetry

5.2.1. Longitudinal waves propagating along symmetry axes

Let us consider a wave propagating along the direction \mathbf{m}_0 , which coincides with a symmetry axis of any order except for dyad axes (e.g., this can be the 3, 4, $\bar{4}$, 6, or $\bar{6}$ -fold axis). As is known (Fedorov, 1968), any symmetry axis (including a dyad axis) is a longitudinal normal. Evidently, the electric induction $\mathbf{D}_l(\mathbf{m}_0)$ accompanying the longitudinal wave ($\mathbf{u}_l \parallel \mathbf{m}_0$) must be zero, otherwise the $\mathbf{D}_l(\mathbf{m}_0)$ vector would possess two equivalent orientations, in contradiction with the single-valued third relation in (9):

$$\mathbf{D}_l = ik\hat{N}(\mathbf{m}_0)\mathbf{m}_0. \quad (39)$$

It should be noted that this argument does not work in the case of transverse branches. For the selected symmetry directions they are always degenerate, that is, possessing equal phase velocities ($v_t = v_{t'}$) and, hence, arbitrary orientations of $\mathbf{u}_{t,t'}$ and $\mathbf{D}_{t,t'}$ in the plane:

$$\{\mathbf{u}_{t,t'}, \mathbf{D}_{t,t'}\} \perp \mathbf{m}_0. \quad (40)$$

The wave propagating along a dyad axis should be treated separately (albeit with the same result). In the general case, this direction is not an acoustic axis. On the other hand, the transverse isonormal vectors $\mathbf{D}_a \perp \mathbf{m}_0$ ($a = t, t', l$) are determined to within the sign (like \mathbf{u}_a) and, hence, their symmetry rotations due to the dyad axis cannot be considered as different solutions. So, one can readily check that, for a propagation direction along the dyad axis, the transverse branches $a = t, t'$ are again characterized by nonzero induction vectors. However, the longitudinal branch in the same direction always obeys the relation $\mathbf{D}_l(\mathbf{m}_0) = 0$. Indeed, combining Eqs. (10) and (39) for $\mathbf{m} = \mathbf{m}_0$, we obtain

$$\mathbf{D}_l / ik = \hat{N}(\mathbf{m}_0)\mathbf{m}_0 = (\hat{\mathbf{e}}\mathbf{m}_0)\mathbf{m}_0 - \frac{(\hat{\mathbf{e}}\mathbf{m}_0)[(\mathbf{m}_0\hat{\mathbf{e}}\mathbf{m}_0)\mathbf{m}_0]}{\mathbf{m}_0 \cdot \hat{\mathbf{e}}\mathbf{m}_0}. \quad (41)$$

Let us check that the right-hand part of this expression vanishes even for a monoclinic crystal of the class 2. Selecting the z axis in (41) along the dyad axis ($2 \parallel \mathbf{m}_0$), we obtain

$$\mathbf{D}_l / ik = \left(e_{13} - \frac{\varepsilon_{13}e_{33}}{\varepsilon_{33}}, \quad e_{23} - \frac{\varepsilon_{23}e_{33}}{\varepsilon_{33}}, \quad 0 \right). \quad (42)$$

However, according to (Royer & Dieulesaint, 2000; Sirotin & Shaskolskaya, 1982), the off-diagonal components of $\hat{\varepsilon}$ and $\hat{\mathbf{e}}$ tensors, entering into Eq. (42) for the symmetry class 2 in this coordinate system, are vanishing: $e_{13} = e_{23} = \varepsilon_{13} = \varepsilon_{23} = 0$ and, hence,

$$\mathbf{D}_l(\mathbf{m}_0 \parallel 2) = 0. \quad (43)$$

Evidently, Eq. (43) is valid for all crystals of various classes possessing dyad axes. Thus, the following statement is valid:

A longitudinal wave propagating along any axis of symmetry in a piezoelectric crystal is accompanied by an electric component with zero induction.

For example, let us consider a piezoelectric crystal of the orthorhombic symmetry class 222. According to the above theorem, all three dyad axes in this crystal are the zero-induction directions \mathbf{m}_0 for the longitudinal modes. However, it can be shown that another four inversion-nonequivalent asymmetric directions \mathbf{m}_0 with zero induction ($\mathbf{D}_l = 0$) may exist in a quasi-longitudinal branch of this crystal:

$$(\theta_0, \pm \varphi_0), (\theta_0, \pm \varphi_0 + \pi), \quad (44)$$

where the angles of spherical coordinate system are determined by approximate relations

$$\theta_0 = \operatorname{arccot} \sqrt{\frac{e_{36} \varepsilon_1 \varepsilon_2}{(e_{14} \varepsilon_2 + e_{25} \varepsilon_1) \varepsilon_3}}, \quad \varphi_0 = \arctan \sqrt{\frac{e_{25} \varepsilon_1}{e_{14} \varepsilon_2}}. \quad (45)$$

For simplicity, solutions (45) are written in the approximation of small piezoelectric moduli and weak elastic anisotropy. In this approximation, a necessary condition for the existence of the above series of zero induction points is that all the piezoelectric moduli entering into relations (45) must have the same sign (Fig. 2). It should be noted that cubic piezoelectric crystals (symmetry classes $\bar{4}3m$ and 23) are always described by Fig. 2b, since additional zero-induction directions (44), (45) always appear along the triad axes.

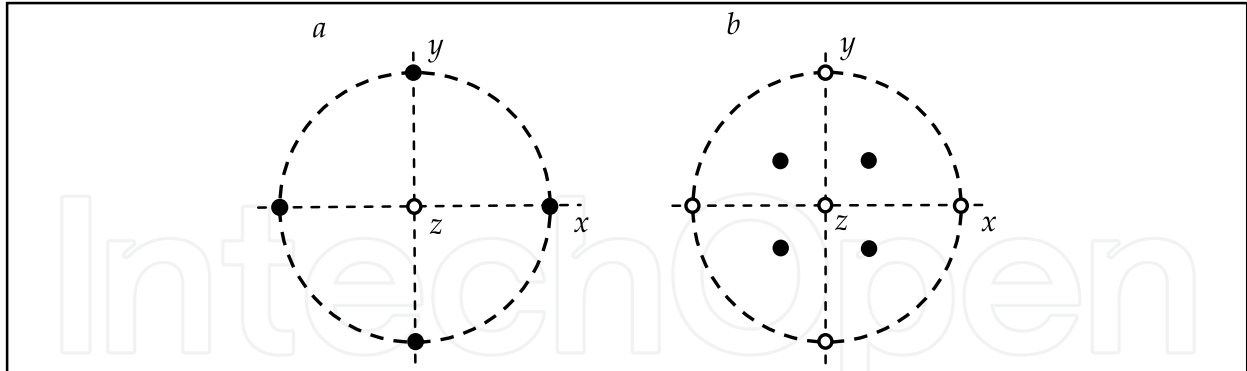


Figure 2. Diagrams of the directions of propagation of the transversely nonpiezoactive acoustic waves of quasi-longitudinal branch in crystals of the symmetry class 222. The stereographic projections are given for the cases when (a) the sign of the piezoelectric modulus e_{36} is opposite to that of e_{14} and/or e_{25} and (b) all piezoelectric moduli have the same sign.

5.2.2. Transverse (SH) waves propagating in symmetry planes

Example 1: symmetry class m . Let the z axis be perpendicular to the plane of symmetry of a monoclinic crystal ($z \perp m$) and consider the t branch of a wave propagating in this plane:

$$\mathbf{m} = (m_1, m_2, 0), \quad \mathbf{u}_t \parallel (0, 0, 1). \quad (46)$$

One can readily check that in such waves

$$\mathbf{D}_t \parallel (0, 0, e_{35}m_1 + e_{34}m_2)u_t \parallel \mathbf{u}_t. \quad (47)$$

Therefore, the symmetry plane always contains a single direction \mathbf{m}_0 corresponding to zero induction \mathbf{D}_t , which is determined by the azimuthal angle φ_0 (counted as in Fig. 1):

$$\mathbf{m}_0 = (m_{01}, m_{02}, 0), \quad \tan \varphi_0 = m_{02} / m_{01} = -e_{35} / e_{34}. \quad (48)$$

The maximum amplitude of \mathbf{D}_t in this plane corresponds to the direction

$$\mathbf{m}_{\max} = (m_{02}, -m_{01}, 0), \quad (49)$$

which is perpendicular to \mathbf{m}_0 .

This is the most general example. Thus, the following theorem is valid:

In any symmetry plane there is always at least one direction for propagation of an SH wave with vanishing electric induction.

The other examples below just specify orientations of the zero-induction direction in various symmetry classes.

Example 2: symmetry class $3m$. In trigonal crystals, the situation with transverse nonpiezoactive directions for the t waves in each of the three symmetry planes containing the triad axis is completely analogous to the above case of a monoclinic crystal. For example, in the yz symmetry plane, relations (46)–(48) have to be replaced by

$$\mathbf{m} = (0, m_2, m_3), \quad \mathbf{u}_t \parallel (1, 0, 0), \quad (50)$$

$$\mathbf{D}_t \parallel (-e_{22}m_2 + e_{15}m_3, 0, 0)u_t \parallel \mathbf{u}_t, \quad (51)$$

$$\mathbf{m}_0 = (0, m_{02}, m_{03}), \quad \tan \theta_0 = \frac{m_{02}}{m_{03}} = \frac{e_{15}}{e_{22}} \quad (52)$$

where θ_0 is the polar angle between \mathbf{m}_0 and the triad axis.

Example 3: symmetry class $mm2$. For a t wave propagating in the yz symmetry plane of an orthorhombic crystal, we have

$$\begin{aligned} \mathbf{m} &= (0, m_2, m_3), \quad \mathbf{u}_t \parallel (1, 0, 0), \\ \mathbf{D}_t &\parallel (e_{15}m_3, 0, 0)u_t \parallel \mathbf{u}_t. \end{aligned} \quad (53)$$

Evidently, in this case

$$\mathbf{m}_0 = (0, 1, 0), \quad \mathbf{m}_{\max} = (0, 0, 1). \quad (54)$$

Relations (53) and (54) are also valid for tetragonal crystals of the symmetry class $4mm$.

Example 4: symmetry classes $\bar{4}2m$, $\bar{4}3m$, and 23. For the x axis parallel to the dyad axis ($x \parallel 2$), transverse waves propagating in the diagonal plane $(1, \bar{1}, 0)$ obey the relations

$$\mathbf{m} = (m_1, -m_1, m_3), \quad \mathbf{u}_t \parallel (1, 1, 0). \quad (55)$$

These waves exhibit electric components with the amplitude of induction

$$\mathbf{D}_t \parallel e_{14}m_3(1, 1, 0)\mathbf{u}_t \parallel \mathbf{u}_t \quad (56)$$

and, hence, have the following special directions:

$$\mathbf{m}_0 = (1, -1, 0)/\sqrt{2}, \quad \mathbf{m}_{\max} = (0, 0, 1). \quad (57)$$

The found above orientations of zero-induction direction \mathbf{m}_0 for a series of crystal classes are summarized in Table 2.

| Class of symmetry | m | $3m$ | $mm2, 4mm$ | $\bar{4}2m, \bar{4}3m, 23$ |
|--------------------------|--|---|----------------------------|--------------------------------------|
| Symmetry plane | $m \perp z$ | $m \parallel yz$ | $m \parallel yz$ | $m \parallel (1\bar{1}0)$ |
| Direction \mathbf{m}_0 | $\mathbf{m}_0 = (m_{01}, m_{02}, 0)$ $m_{02} / m_{01} = -e_{35} / e_{34}$ | $\mathbf{m}_0 = (0, m_{02}, m_{03})$ $m_{02} / m_{03} = e_{15} / e_{22}$ | $\mathbf{m}_0 = (0, 1, 0)$ | $\mathbf{m}_0 = (1, -1, 0)/\sqrt{2}$ |

Table 2. Propagation directions of transversely nonpiezoactive SH waves in the symmetry planes of crystals of various symmetry systems. Certainly, in Table 2 for crystals more symmetric than monoclinic (m) and containing other equivalent symmetry planes, the directions \mathbf{m}_0 of zero induction found are accordingly multiplied. For instance, in crystals of the orthorhombic ($mm2$) and tetragonal ($4mm$) classes there is also the symmetry plane $m \parallel xz$ where the corresponding transversely non-piezoactive direction is $\mathbf{m}_0 = (1, 0, 0)$.

In conclusion, let us consider the more exclusive case of hexagonal symmetry classes (14).

Example 5: symmetry classes $6mm$ and ∞m (14). Any plane containing the principal symmetry axis in such a crystal is the plane of symmetry m . According to relations (27), the electric induction vector of t waves propagating in such planes is orthogonal to m and proportional to m_3 . Therefore, \mathbf{D}_t vanishes along the entire equator $m_3 = 0$:

$$\mathbf{D}_t(m_1, m_2, 0) = 0. \quad (58)$$

Note in passing that at the same equator for the same symmetry classes the other transverse branch (t') polarized along the principal axis also forms a line of zero electric displacement:

$$\mathbf{D}_{t'}(m_1, m_2, 0) = 0. \quad (59)$$

6. Orientational singularities of the induction fields

The vector fields $\mathbf{D}_a(\mathbf{m})$, which are orthogonal to the wave normal \mathbf{m} , may exhibit orientational singularity in the vicinity of directions of the two types: zero-induction points, where rotations are topologically allowed (Alshits, Lyubimov & Radowicz, 2005a, 2005b), and along acoustic axes, where inductions of degenerate branches, as a rule, do not vanish, but rotate together with the corresponding displacement vectors \mathbf{u}_{0a} (Alshits *et al.*, 1987).

Below we shall consider the both types of singularities concentrating our attention basically on the directions of transverse nonpiezoactivity.

6.1. General case of arbitrary anisotropy

6.1.1. Orientational singularities in the vicinities of zero-induction points

As was mentioned above, the vector fields $\mathbf{D}_a(\mathbf{m})$ in the zero-induction points \mathbf{m}_0 may exhibit rotations (Fig 3). Let us consider the $\mathbf{D}_a(\mathbf{m})$ function for $\mathbf{m} = \mathbf{m}_0 + \Delta\mathbf{m}$, where $\Delta\mathbf{m} \perp \mathbf{m}_0$ and $|\Delta\mathbf{m}| \ll 1$. Using condition (8) and the third relation in (9), we obtain

$$\mathbf{D}_a(\mathbf{m}) \parallel \hat{N}(\mathbf{m}) \bar{\hat{F}}_a(\mathbf{m}) \mathbf{c}. \quad (60)$$

Taking into account that $\mathbf{D}_a(\mathbf{m}_0) = 0$, one has from (60) to a first approximation:

$$\mathbf{D}_a(\mathbf{m}) \parallel \Delta\mathbf{m} \hat{Q}_a \equiv \Delta m_i \left\{ \frac{\partial}{\partial m_i} [\hat{N}(\mathbf{m}) \bar{\hat{F}}_a(\mathbf{m}) \mathbf{c}] \right\}_{\mathbf{m}=\mathbf{m}_0}. \quad (61)$$

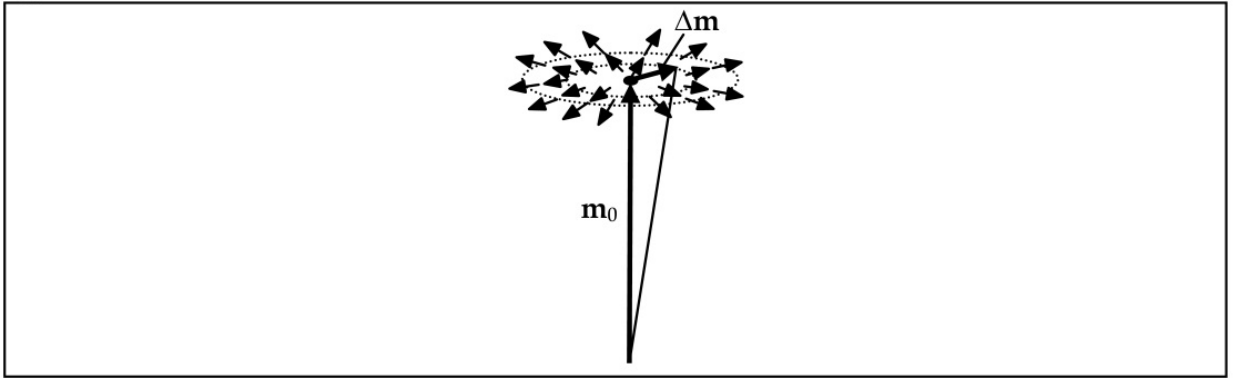


Figure 3. A singular vector distribution $\mathbf{D}_a(\mathbf{m})$ in the vicinity of a zero-induction point \mathbf{m}_0 .

For the transverse $\mathbf{D}_a(\mathbf{m})$ field [see (11)], the asymmetric tensor entering into formula (61),

$$\hat{Q}_a = \nabla_{\mathbf{m}} \otimes \hat{N}(\mathbf{m}) \bar{\hat{F}}_a(\mathbf{m}) \mathbf{c} |_{\mathbf{m}=\mathbf{m}_0}, \quad (62)$$

must be planar, that is, its spectral expansion can be represented as a sum of two dyads:

$$\hat{Q}_a = \lambda_{a1} \tilde{\mathbf{e}}_{a1} \otimes \mathbf{e}_{a1} + \lambda_{a2} \tilde{\mathbf{e}}_{a2} \otimes \mathbf{e}_{a2}, \quad (63)$$

where λ_{aj} , $\tilde{\mathbf{e}}_{aj}$, and \mathbf{e}_{aj} are the eigenvalues and eigenvectors (left and right) of the \hat{Q}_a tensor (\mathbf{e}_{a1} and \mathbf{e}_{a2} must be orthogonal to \mathbf{m}_0). Note that the $\tilde{\mathbf{e}}_{aj}$ eigenvectors (in contrast to \mathbf{e}_{aj}) in the general case do not belong to a plane orthogonal to \mathbf{m}_0 , but their components $\tilde{\mathbf{e}}_{aj}^{\perp}$ oriented along \mathbf{m}_0 are insignificant for our analysis.

Let us decompose each eigenvector into two components

$$\tilde{\mathbf{e}}_{aj} = \tilde{\mathbf{e}}_{aj}^{\parallel} + \tilde{\mathbf{e}}_{aj}^{\perp}, \quad \tilde{\mathbf{e}}_{aj}^{\parallel} \parallel \mathbf{m}_0, \quad \tilde{\mathbf{e}}_{aj}^{\perp} = (\hat{I} - \mathbf{m}_0 \otimes \mathbf{m}_0) \tilde{\mathbf{e}}_{aj} \perp \mathbf{m}_0, \quad (64)$$

and form a more convenient matrix

$$\hat{Q}_a^{\perp} = (\hat{I} - \mathbf{m}_0 \otimes \mathbf{m}_0) \hat{Q}_a = \lambda_{a1} \tilde{\mathbf{e}}_{a1}^{\perp} \otimes \mathbf{e}_{a1} + \lambda_{a2} \tilde{\mathbf{e}}_{a2}^{\perp} \otimes \mathbf{e}_{a2}, \quad (65)$$

which will be used below instead of \hat{Q}_a :

$$\mathbf{D}_a \parallel \Delta \mathbf{m} \hat{Q}_a^{\perp}. \quad (66)$$

Let the orientation angle Φ of the $\mathbf{D}_a(\mathbf{m})$ vector be measured from the \mathbf{e}_{a1} direction, and the analogous angle φ for $\Delta \mathbf{m}$ in the same plane, from the $\tilde{\mathbf{e}}_{a1}^{\perp}$ direction (Fig. 4). In these terms, we can write

$$\tan \Phi = \frac{\mathbf{D}_a \cdot \mathbf{e}_{a2}}{\mathbf{D}_a \cdot \mathbf{e}_{a1}} = \frac{\lambda_{a2}}{\lambda_{a1}} \frac{\Delta \mathbf{m} \cdot \tilde{\mathbf{e}}_{a2}^{\perp}}{\Delta \mathbf{m} \cdot \tilde{\mathbf{e}}_{a1}^{\perp}} = \frac{\lambda_{a2}}{\lambda_{a1}} \tan \varphi. \quad (67)$$

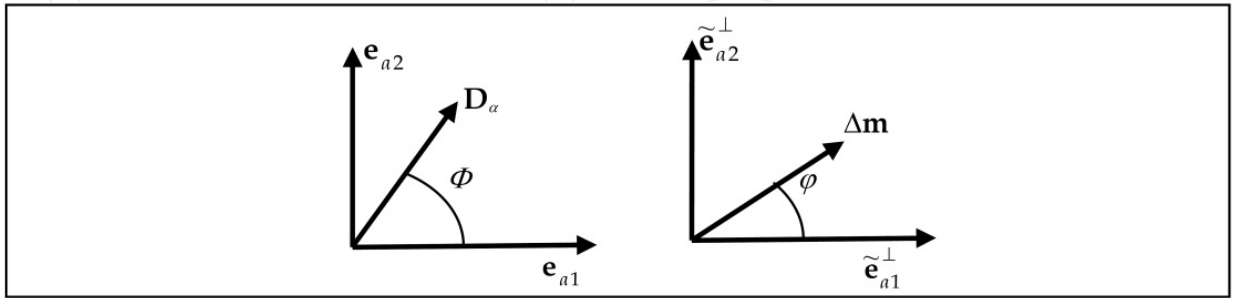


Figure 4. The angles of orientation of the \mathbf{D}_a and $\Delta \mathbf{m}$ vectors in the plane orthogonal to \mathbf{m}_0 .

Thus, the complete turn of $\Delta \mathbf{m}$ around \mathbf{m}_0 in the plane orthogonal to \mathbf{m}_0 implies the complete turn of $\mathbf{D}_a(\mathbf{m})$ in the same or in the opposite direction (depending on the sign of $\det \hat{Q}_a^{\perp} = \lambda_{a1} \lambda_{a2}$), which corresponds to the Poincaré index of the given singular point (Fig. 5)

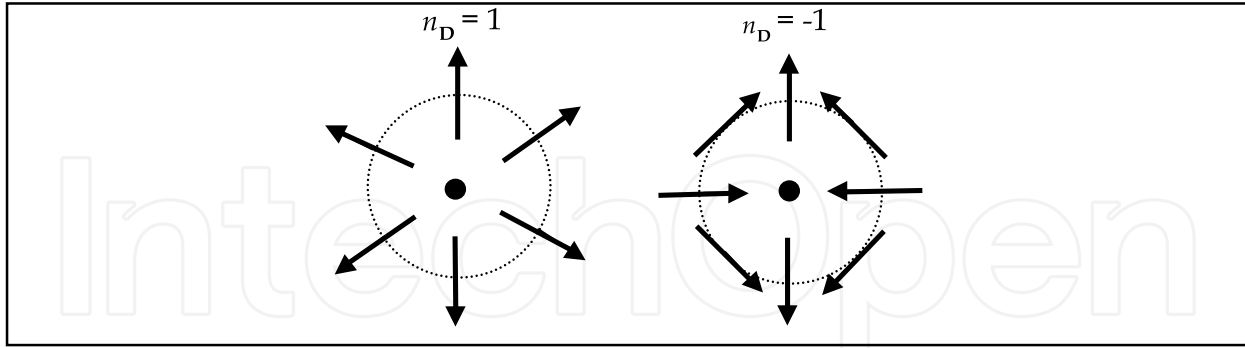


Figure 5. The two main types of singularities in the vicinity of zero points of the induction vector distribution in the normalized directed representation.

$$n_D = \text{sgn det} \hat{Q}_a^\perp. \quad (68)$$

The above considerations fail to be valid in particular cases, when one of the eigenvalues (λ_{a1} or λ_{a2}) of matrices (63) and (65) vanishes. In such cases, $\text{det} \hat{Q}_a^\perp = 0$, but formula (68) is not applicable. Indeed, let $\lambda_{a2} = 0$ at \mathbf{m}_0 . Then,

$$\mathbf{D}_a \parallel \Delta \mathbf{m} \hat{Q}_a^\perp = \lambda_{a1} (\Delta \mathbf{m} \cdot \tilde{\mathbf{e}}_{a1}^\perp) \mathbf{e}_{a1} \quad (69)$$

and a zero-induction line can pass via \mathbf{m}_0 in the direction of $\Delta \mathbf{m} \perp \tilde{\mathbf{e}}_{a1}^\perp$, but only provided that $\lambda_{a2} = 0$ is valid. In this situation, the very concept of the Poincaré index is inapplicable. However, if the vanishing of λ_{a2} has a strictly local character and takes place only along \mathbf{m}_0 , then we are dealing with a very special singularity analogous to a local-wedge degeneracy known in the theory of acoustic axes (Alshits, Sarychev & Shuvalov, 1985). It can be shown that a topological charge of the corresponding singularity in the $\mathbf{D}_a(\mathbf{m})$ field in this case can take one of three values: $n_D = 0, \pm 1$. However, both situations (point and line) of this type with zero induction amplitude are very exclusive and never encountered in real (even symmetric) crystals. Below we will consider zero-induction lines of this kind in model crystals. However it will be demonstrated that the examples of the $\mathbf{D}_a = 0$ lines, existing in hexagonal crystals and described by Eqs. (58) and (59), belong to a different type.

On the other hand, the ordinary singular points (68) with indices $n_D = \pm 1$ depicted in Fig. 5 are rather widely encountered in real crystals. For example, all directions \mathbf{m}_0 in Fig. 2b corresponding to orthorhombic (222) or cubic ($\bar{4}3m$ and 23) crystals are characterized by topological charges $n_D = \pm 1$ (in Fig. 2, filled and empty circles correspond to +1 and -1, respectively). Figure 6 is a schematic diagram of the $\mathbf{D}_l(\mathbf{m})$ distribution in the central region of the circle in Fig. 2b.

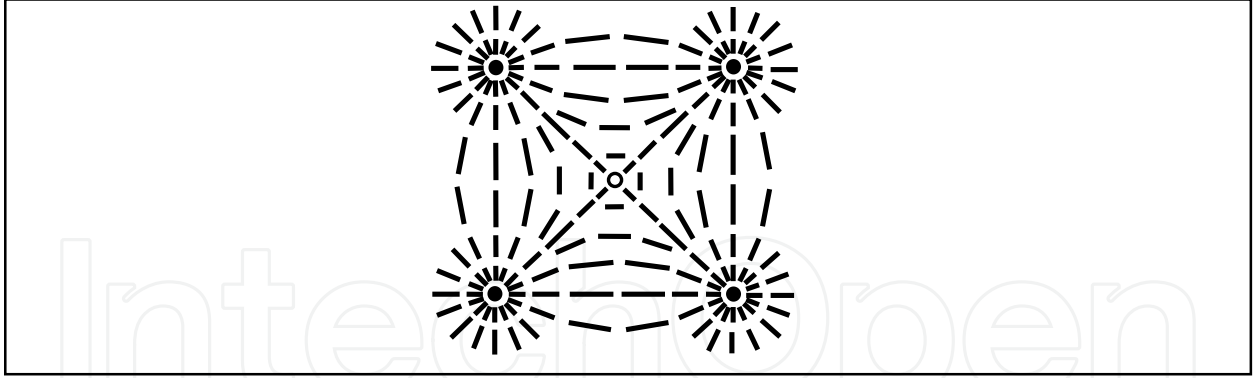


Figure 6. A schematic image of the $\mathbf{D}_l(\mathbf{m})$ vector field distribution over a group of five singular points in the central region of Fig. 2b in the representation of nondirected segments.

6.1.2. Orientational singularities in the $\mathbf{D}_a(\mathbf{m})$ fields around acoustic axes

Let us consider the vector polarization fields $\mathbf{u}_{01,2}(\mathbf{m})$ of degenerate branches in the vicinity of the direction \mathbf{m}_d of the acoustic axis. In this region the considered vector distributions should be very close to the plane orthogonal to the unit polarization vector $\mathbf{u}_{03}(\mathbf{m}_d)$ of the non-degenerate isonormal eigenwave being singular at \mathbf{m}_d . Their rotations around the acoustic axis are equal to each other being described by the Poincaré index n_u which is determined by the type of the acoustic axis (Alshits *et al*, 1987). The appropriate fields of electric induction $\mathbf{D}_{1,2}(\mathbf{m})$ due to the coupling (9) $\mathbf{D}_a \parallel \hat{N}\mathbf{u}_a$ have similar rotations characterized by the Poincaré index n_D which ordinarily may differ from n_u only by a sign. In order to find this sign we should take into consideration that the \hat{N} matrix is degenerate ($\mathbf{m}\hat{N} = 0$). However, one can replace \hat{N} by a matrix \hat{N}' such that we have $\hat{N}'\mathbf{u} = \hat{N}\mathbf{u}$ for any $\mathbf{u} \perp \mathbf{u}_{03}$, but simultaneously $\det \hat{N}' \neq 0$. These conditions are satisfied by, for example, the matrix

$$\hat{N}' = \hat{N}(\mathbf{m}_d) + \mathbf{m}_d \otimes \mathbf{u}_{03}. \quad (70)$$

Indeed, in accordance with (Fedorov, 1968) we have $\det \hat{N}' = \mathbf{u}_{03} \cdot \hat{N}\mathbf{m}_d \neq 0$. Then following to (Alshits *et al*, 1987) one obtains

$$n_D = n_u \operatorname{sgn} \det \hat{N}'. \quad (71)$$

This equation is valid until $\hat{N}(\mathbf{m}_d) \neq 0$ which holds for any known acoustic axes except of the direction $\mathbf{m}_d \parallel \bar{6}$ (see below).

It should be noted that, in contrast to the mutually orthogonal vectors $\mathbf{u}_{0a}(\mathbf{m})$ ($a = 1, 2, 3$), the three vectors $\mathbf{D}_a(\mathbf{m}) \perp \mathbf{m}$ are coplanar and generally unorthogonal in pairs. At the same time, it is clear that the vectors $\mathbf{D}_1(\mathbf{m})$ and $\mathbf{D}_2(\mathbf{m})$ are not collinear with any \mathbf{m} .

Consequently, these two vector fields are homotopic with each other. That is why they correspond to the same value of the index n_D .

Now let us consider some examples of crystals belonging to particular symmetry systems.

6.2. Waves propagating along symmetry axes

6.2.1. Longitudinal waves along symmetry axes

Example 1. For a longitudinal wave propagating along the $\mathbf{m}_0 \parallel 2$ direction in a monoclinic crystal with dyad axis, we have

$$n_D = \text{sgn}\{(a_1 + b_1)(a_2 + b_2) - c_1 c_2\}. \quad (72)$$

where

$$a_1 = \frac{e_{14} c_{36}}{\Delta_{34}^-}, \quad b_1 = \frac{e_{15} d_1}{\Delta_{35}^-} - \frac{e_{33} \varepsilon_1}{\varepsilon_3}, \quad c_1 = \frac{e_{14} d_2}{\Delta_{34}^-} + \frac{e_{15} c_{36}}{\Delta_{35}^-}, \quad (73)$$

$$a_2 = \frac{e_{25} c_{36}}{\Delta_{35}^-}, \quad b_2 = \frac{e_{24} d_2}{\Delta_{34}^-} - \frac{e_{33} \varepsilon_2}{\varepsilon_3}, \quad c_2 = \frac{e_{25} d_1}{\Delta_{35}^-} + \frac{e_{24} c_{36}}{\Delta_{34}^-}, \quad (74)$$

$d_i = c_{i3} + c_{33}$. The $\hat{\varepsilon}$ tensor is assumed to be diagonal, which can be ensured by the appropriate choice of the x - and y axes of the crystallographic coordinate system with the z axis parallel to the dyad axis.

Example 2. For the $\mathbf{m}_0 \parallel 2$ direction in an orthorhombic crystal belonging to the symmetry class $mm2$, we have

$$n_D = \text{sgn}(b_1 b_2). \quad (75)$$

Example 3. For the $\mathbf{m}_0 \parallel 2 \parallel z$ direction in an orthorhombic crystal belonging to the symmetry class 222 , we have

$$n_D^{(z)} = \text{sgn}(a_1 d_2 / a_2 d_1). \quad (76)$$

Analogous formulas for the $n_D^{(x)}$ and $n_D^{(y)}$ are obtained from (76) by cyclic rearrangement of the indices. Note that, in the isotropic limit, we obtain

$$d_1 / \Delta_{35}^- = d_2 / \Delta_{34}^- \rightarrow 2, \quad (77)$$

and only a very large elastic anisotropy can change the signs of the ratios in formula (76). Therefore these signs for most orthorhombic crystals are determined only by the piezoelectric moduli: $n_D^{(z)} = \text{sgn}(e_{14} e_{25})$.

Example 4. As can be readily checked, for the principal symmetry axes in crystals of the symmetry classes 422 , 622 , $\infty 22$, $4mm$, $6mm$, ∞mm , 4 , 6 , ∞ , 32 , $3m$, and 3 we have

$$n_D = 1, \quad (78)$$

and in crystals of the symmetry classes $\bar{4}2m$, $\bar{4}$, $\bar{4}3m$, and 23 ,

$$n_D = -1. \quad (79)$$

6.2.2. Degenerate transverse waves along symmetry axes

In accordance with Eq. (71), the transverse waves propagating along directions near acoustic axes, which coincide with symmetry axes in piezoelectric crystals, are characterized by rotations of both polarization fields $\mathbf{u}_{01,2}(\mathbf{m})$ and accompanied induction fields $\mathbf{D}_{1,2}(\mathbf{m})$.

The direct analysis for various types of symmetry axes gives the related Poincaré indices n_u and n_D shown in Table 3.

| N | $\infty, 6$ | | $\bar{6}$ | | 4 | | $\bar{4}$ and $2 \in 23$ | | 3 | |
|--------|-------------|------|-----------|------|---------|------|--------------------------|------|-------|------|
| branch | trans | long | trans | long | trans | long | trans | long | trans | long |
| n_u | 1 | 0 | 1 | 0 | ± 1 | 0 | ± 1 | 0 | -1/2 | 0 |
| n_D | 1 | 1 | -2 | -2 | n_u | 1 | $-n_u$ | -1 | -1/2 | 1 |

Table 3. The Poincaré indices of vector fields of polarizations and inductions along acoustic axes coinciding with symmetry axes N for transverse and longitudinal wave branches. The sign of $n_u = \pm 1$ when it is not universal may be found from the equations given in (Alshits, Sarychev & Shuvalov, 1985; Alshits & Shuvalov, 1987; Shuvalov, 1998). The indices n_D for the direction of a $\bar{6}$ -fold symmetry axis are found in the next sub-section.

6.2.3. The both types of induction singularities along a $\bar{6}$ -fold symmetry axis

An interesting configuration of the vector fields $\mathbf{D}_a(\mathbf{m})$ arises near an acoustic axis $\mathbf{m}_d \parallel \bar{6}$. In this case we have an exclusive situation $\hat{N}(\mathbf{m}_d) = 0$. So, by Eq. (9)₃, along the direction \mathbf{m}_d the induction components vanish, $\mathbf{D}_a(\mathbf{m}_d) = 0$, in all branches, both degenerate ($a = 1, 2 \equiv t, t'$) and nondegenerate ($a = 3 \equiv l$). Accordingly, in the vicinity of the $\bar{6}$ -fold symmetry axis these fields should be small. Let us consider the direction

$$\mathbf{m} = \mathbf{m}_d + \Delta \mathbf{m} \quad (80)$$

where

$$\begin{aligned} \mathbf{m}_d &= (0, 0, 1) \parallel \bar{6}, & \Delta \mathbf{m} &= \mu \boldsymbol{\rho}(\varphi), \\ \boldsymbol{\rho}(\varphi) &= (\cos \varphi, \sin \varphi, 0), & 0 \leq \mu < 1. \end{aligned} \quad (81)$$

In these terms, the vector fields $\mathbf{D}_a(\mathbf{m})$, in the main order, have the following form

$$\begin{aligned} \mathbf{D}_l &= \mu^2(d / \Delta_{34})\{e_{11}\boldsymbol{\rho}(-2\varphi) + e_{22}[\boldsymbol{\rho}(-2\varphi) \times \mathbf{m}_0]\}, \\ \mathbf{D}_t &= \mu\{e_{22}\boldsymbol{\rho}(-2\varphi) - e_{11}[\boldsymbol{\rho}(-2\varphi) \times \mathbf{m}_0]\}, \\ \mathbf{D}_{t'} &= \mu\{e_{11}\boldsymbol{\rho}(-2\varphi) + e_{22}[\boldsymbol{\rho}(-2\varphi) \times \mathbf{m}_0]\}. \end{aligned} \quad (82)$$

Here the notation is introduced: $d = c_{13} + c_{44}$, $\Delta_{34} = c_{33} - c_{44}$. We note that in the symmetry classes $\bar{6}m2$ ($m \perp X_1$) and $\bar{6}2m$ ($2 \parallel X_1$) one can put in (82), respectively, $e_{11} = 0$ and $e_{22} = 0$.

It is easily seen that the induction vectors \mathbf{D}_t and $\mathbf{D}_{t'}$ of the degenerate branches are mutually orthogonal, while their absolute value is proportional to $|\Delta\mathbf{m}|$ and does not depend on the orientation φ of the vector $\Delta\mathbf{m}$. The induction vector \mathbf{D}_l of the non-degenerate quasi-longitudinal branch has much smaller length, $|\mathbf{D}_l| \propto |\Delta\mathbf{m}|^2$, which also does not depend on φ . The direction of \mathbf{D}_l in the accepted main order coincides with that of $\mathbf{D}_{t'}$. Certainly, in the next approximation this coincidence disappears. It is clear from (82) that during the full rotation of the vector $\Delta\mathbf{m}$ around the axis $\mathbf{m}_d \parallel \bar{6}$ each of three vectors \mathbf{D}_α twice circumvents the same axis in opposite direction. This means that the point $\mathbf{m}_d \parallel \bar{6}$ in all three vector fields is characterized by the Poincaré index $n_D = -2$ (Table 3). The corresponding singular configuration for one of these vector fields is shown in Fig. 7.

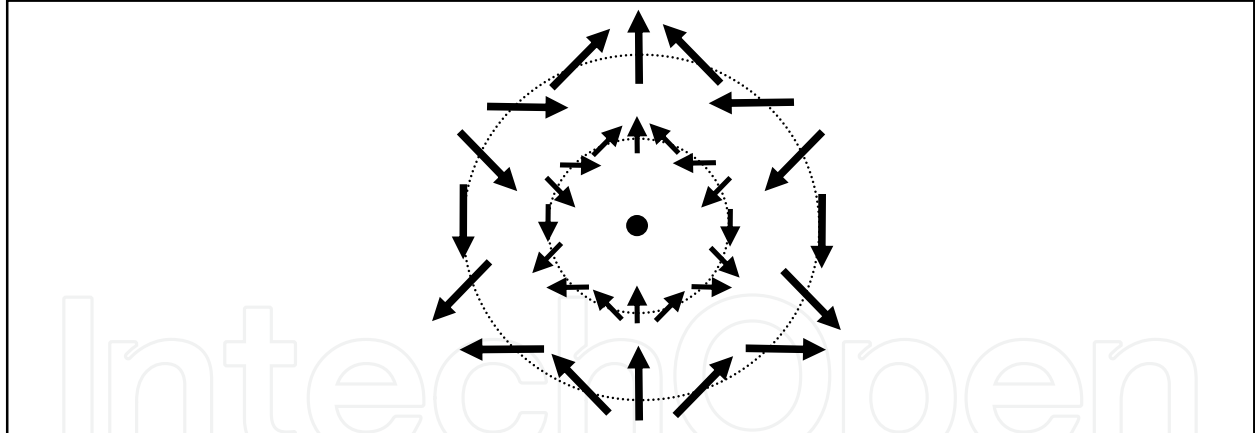


Figure 7. Vector induction field \mathbf{D}_a , $a = t, t'$ or l , near the acoustic axis $\mathbf{m}_d \parallel \bar{6}$ related to the Poincaré index $n_D = -2$ (top view of the plane orthogonal to \mathbf{m}_d ; the central point corresponds to the direction of \mathbf{m}_d).

6.3. Transverse (SH) waves propagating in symmetry planes

The directions of transverse nonpiezoactivity in symmetry planes (Table 2) are also characterized by rotations n_D in the induction vector fields of appropriate SH wave branches. We will not write lengthy expressions determining the choice between $n_D = \pm 1$

indices for the waves along \mathbf{m}_0 directions in monoclinic and trigonal crystals (see relations (49) and (52), respectively) and instead start our analysis from orthorhombic crystals.

Example 1. For the transverse acoustic waves (53) and (54) propagating in the vicinity of the zero-induction direction $\mathbf{m}_0 = (0, 1, 0)$ in an orthorhombic crystal belonging to the symmetry class $mm2$, the singular induction field is characterized by the Poincaré index

$$n_D = \text{sgn} \left[\frac{e_{32}(c_{12} + c_{66}) / \Delta_{26}^- - e_{31}}{e_{15}} \right] \quad (83)$$

Example 2. For the same direction in a tetragonal crystal belonging to the symmetry class $4mm$, we have

$$n_D = \text{sgn} \left[\frac{e_{31}(c_{12} - c_{11} + 2c_{66})}{e_{15}\Delta_{16}^-} \right] \quad (84)$$

Example 3. For the direction $\mathbf{m}_0 = (1, -1, 0) / \sqrt{2}$ in a crystal belonging to the other tetragonal symmetry class $\bar{4}2m$, we obtain

$$n_D = -\text{sgn}(e_{14} / e_{36}). \quad (85)$$

Example 4. For the same direction in a cubic crystals of the symmetry class $\bar{4}3m$ or 23 in the diagonal symmetry plane, as well as for the symmetry-equivalent direction $\mathbf{m}_0 = (-1, 1, 0) / \sqrt{2}$, we have (for any combinations of the moduli)

$$n_D = -1 \quad (86)$$

The results presented in this subsection are summarized in Table 4.

| Classes of symmetry | $mm2$ | $4mm$ | $\bar{4}2m$ | $\bar{4}3m, 23$ |
|--------------------------|--|--|--|-----------------|
| Symmetry plane | $m \parallel yz$ | | $(1\bar{1}0)$ | |
| Direction of propagation | $\mathbf{m}_0 = (0, 1, 0)$ | | $\mathbf{m}_0 = (1, -1, 0) / \sqrt{2}$ | |
| Poincare index n | $\text{sgn} \left(\frac{e_{32}}{e_{15}} \kappa_2 - \frac{e_{31}}{e_{15}} \right)$ | $\text{sgn} \left(\frac{e_{31}}{e_{15}} (\kappa_1 - 1) \right)$ | $\text{sgn} \left(-\frac{e_{14}}{e_{36}} \right)$ | -1 |

Table 4. Topological charges of \mathbf{D} fields for SH acoustic waves propagating in symmetry planes of various crystals. In this table the notation is introduced:

$$\kappa_p = \frac{c_{12} + c_{66}}{c_{pp} - c_{66}} \quad (87)$$

6.4. Special types of singularities

The general analysis in Sec. 6.1 is exhaustive only provided that the \hat{Q}_a tensor (62) is nonzero. As was shown above, usual systems have $\hat{Q}_a \neq 0$. However, in some very exclusive cases, this tensor may vanish in some special directions because of high symmetry or as a result of vanishing of certain combinations of the material tensor components. In such cases, the general expressions are very lengthy and we only present here some final results. For $\hat{Q}_a(\mathbf{m}_0) = 0$, the distribution of the induction vector field in the vicinity of \mathbf{m}_0 has four additional variants depicted in Fig. 8. The first three of them correspond to isolated singular points with the Poincaré indices $n_D = 0, \pm 2$ (Figs. 8a–8c), while the fourth variant corresponds to the existence of a $\mathbf{D} = 0$ line passing via the \mathbf{m}_0 point (Fig. 8d). This very situation is observed on the equator $m_3 = 0$ for the transverse tangentially polarized t waves (58) in all transverse-isotropic media (13)–(15) and for the transverse t' waves (59) polarized along the principal symmetry axis in the media of symmetry classes $6mm$ and ∞m . The only known alternative example of \hat{Q}_a matrix vanishing is offered by a crystal with hexad axis $\bar{6}$. In this case, all three wave branches have along the direction $\bar{6}$ the identical singularities with $n_D = -2$ (Figs. 7 and 8c).

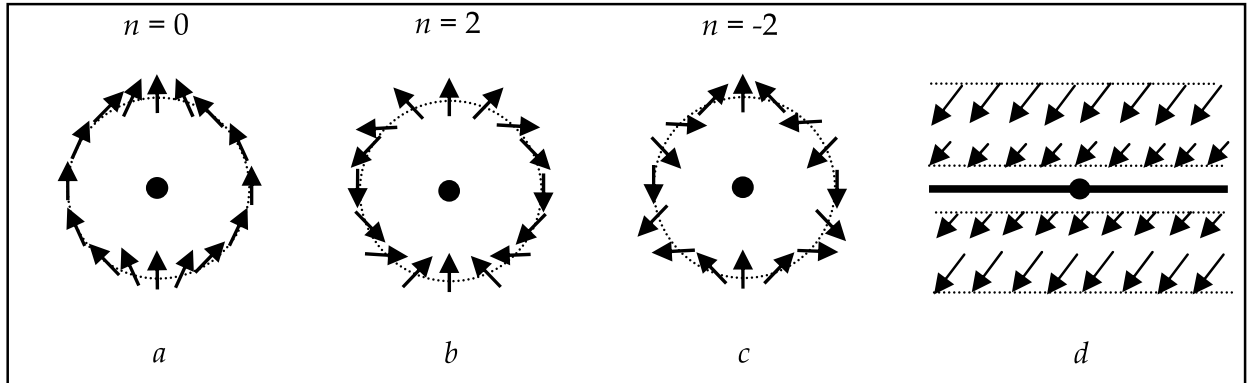


Figure 8. Four possible types of the $\mathbf{D}_a(\mathbf{m})$ vector field distribution around a zero-induction point \mathbf{m}_0 , where $\mathbf{D}_a(\mathbf{m}_0) = \hat{Q}_a(\mathbf{m}_0) = 0$.

6.4.1. A model crystal of the symmetry class $mm2$

Let us assume that one piezoelectric modulus in the crystal under consideration is much smaller than the other moduli. In particular, we consider a conventional crystallographic coordinate system with the x and y axes perpendicular to the symmetry planes and the z axis parallel to the dyad axis, in which

$$|e_{31}| \ll |e_{15}|, |e_{24}|, |e_{32}|, |e_{33}|. \quad (88)$$

One can readily check that, in a zero-order approximation with $e_{31} = 0$, a quasi-longitudinal nondegenerate wave branch along the $\mathbf{m}_0 = (1, 0, 0)$ direction features the above special

situation, whereby simultaneously $\mathbf{D}_l(\mathbf{m}_0) = 0$ and $\hat{Q}_l(\mathbf{m}_0) = 0$. In this case, the $\mathbf{D}_l(\mathbf{m})$ vector field distribution in the yz plane in the vicinity of \mathbf{m}_0 is described by the expression

$$\mathbf{D}_l \parallel \{0, g_2 \sin 2\varphi, g_1 + \varepsilon_1 e_{32} \gamma_2 - (g_1 - \varepsilon_1 e_{32} \gamma_2) \cos 2\varphi\} \quad (89)$$

where φ is a polar angle of the $\Delta \mathbf{m} = \mathbf{m} - \mathbf{m}_0$ direction measured from the y axis in the yz plane and

$$\begin{aligned} g_1 &= \gamma_1 (\varepsilon_1 e_{33} - \varepsilon_3 e_{15}), \\ g_2 &= (\gamma_1 + \gamma_2) \varepsilon_1 e_{24} - \varepsilon_2 e_{15}, \\ \gamma_1 &= \bar{d}_5 / \bar{\Delta}_{15}, \quad \gamma_2 = d_6 / \Delta_{16}, \\ \bar{d}_5 &= c_{13} + \bar{c}_{55}, \quad \bar{\Delta}_{15} = c_{11} - \bar{c}_{55}, \\ \bar{c}_{55} &= c_{55} + e_{15}^2 / \varepsilon_1, \quad d_6 = c_{12} + c_{66}. \end{aligned} \quad (90)$$

Expression (89) shows that, depending on the material constants, the $\mathbf{D}_l(\mathbf{m})$ field always corresponds to one of the possible variants depicted in Fig. 8. The Poincaré indices for the point singularities corresponding to Figs. 8a–8c are as follows:

$$n_l = \begin{cases} 0, & g_1 e_{32} \gamma_2 > 0, \\ 2 \operatorname{sgn}[(g_1 - \varepsilon_1 e_{32} \gamma_2) g_2], & g_1 e_{32} \gamma_2 < 0. \end{cases} \quad (91)$$

A condition for the existence of zero-induction lines in the $\mathbf{D}_l(\mathbf{m})$ field for Fig. 8d is

$$g_1 e_{32} \gamma_2 = 0 \quad \text{or} \quad g_2 = 0, \quad g_1 e_{32} \gamma_2 < 0. \quad (92)$$

According to expression (89), a zero-induction line for $g_1 = 0$ passes via the vector \mathbf{m}_0 along the z axis (Fig. 9a). For $e_{32} \gamma_2 = 0$, a similar zero-induction line is directed along the y axis (Fig. 9b). If $g_1 = 0$ simultaneously with $e_{32} \gamma_2 = 0$, the two lines coexist (Fig. 9c).

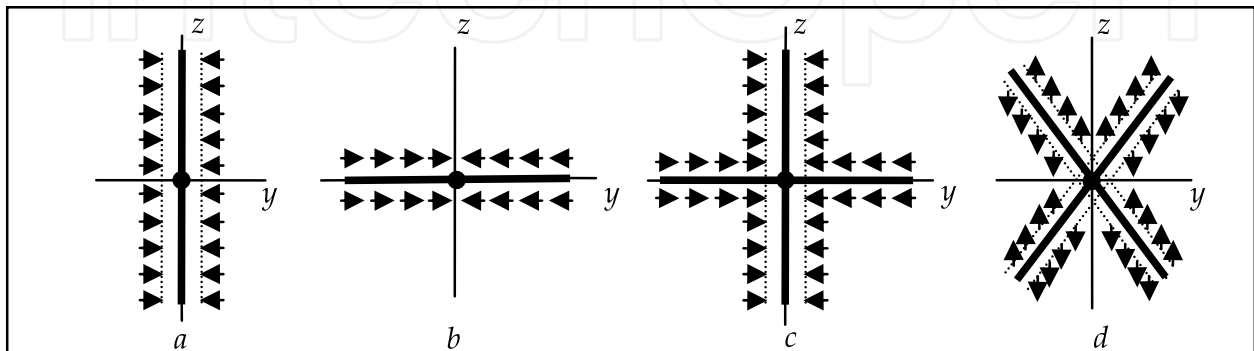


Figure 9. Four possible types of the $\mathbf{D}_l(\mathbf{m}) = 0$ lines in a model orthorhombic crystal.

Finally, when $g_2 = 0$ and $g_1 e_{32} \gamma_2 < 0$, the system features an oblique cross of zero-induction lines (Fig. 9d) with the mutual orientation determined by the equation

$$\cos 2\varphi = \frac{g_1 + \varepsilon_1 e_{32} \gamma_2}{g_1 - \varepsilon_1 e_{32} \gamma_2}. \quad (93)$$

6.4.2. Behavior of point singularities in response to perturbations in the material moduli

The point singularities of various types in vector fields $\mathbf{D}_a(\mathbf{m})$ behave differently in response to perturbations in the material moduli: they shift, split, or disappear. An analysis of this situation, analogous to that carried out by Alshits, Sarychev & Shuvalov (1985), showed that singularities with $n_D = \pm 1$ (Fig. 5) are topologically stable and can only be displaced by such perturbations. The singular points of other types (Figs. 8a–8c) are unstable and either split (in accordance with the law of topological charge conservation) or disappear (provided only that $n_D = 0$). The zero-induction lines (Fig. 8d and Fig. 9) are also unstable and disappear either completely or leaving a certain number of isolated zero points.

Example 1. The above general properties can be illustrated by a particular example using a model crystal of the symmetry class $mm2$ with a small modulus e_{31} described above. It should be recalled that relations (89)–(93) were obtained in the zero-order approximation for $e_{31} = 0$. In the next order with respect to the small parameter e_{31} , the initial singularity along the direction $\mathbf{m}_0 = (1, 0, 0)$ exhibits splitting so as to form two or four singular points:

$$\mathbf{m}_0 + \delta\mathbf{m} = \begin{cases} (1, \pm\mu_2, 0), & \mu_2^2 = -e_{31} / e_{32} \gamma_2, \\ (1, 0, \pm\mu_3), & \mu_3^2 = -e_{31} \varepsilon_1 / g_1. \end{cases} \quad (94)$$

As is seen from Eq.(91) with $g_1 e_{32} \gamma_2 < 0$, the zero-order approximation along \mathbf{m}_0 corresponds to a singularity with $n_D = +2$ or -2 . The introduction of a small e_{31} modulus leads to a symmetric splitting of this singularity into a pair of zero-induction points with equal indices $n_D = +1$ or -1 along the y or z axis, depending on the sign of e_{31} / g_1 (Fig. 10a).

For $g_1 e_{32} \gamma_2 > 0$, when the initial topological charge in the zero-order approximation is zero, the perturbed pattern comprises either four singularities with a zero total index n_D (for $e_{31} / g_1 < 1$) or none of them (which corresponds to the absence of zero-induction points in the vicinity of the given direction for $e_{31} / g_1 > 1$) as depicted in Fig. 10b.

Example 2. It should be noted that the discussed splitting of unstable singularities is by no means reduced to abstract mathematical games. Perturbations in the material moduli of real crystals are frequently caused by various external factors such as electric fields, mechanical stresses, or temperature fluctuations arising in the vicinity of phase transitions. For example, the phase transition from a crystal of the symmetry class $\bar{6}2m$, $\bar{6}m2$, or $\bar{6}$ to a trigonal

crystal of the symmetry class 32 , $3m$, or 3 , respectively, leads to replacement of the hexad axis by a triad axis. Simultaneously, in accordance with Table 3, the polarization singularity $n_u = 1$ in the vector fields \mathbf{u}_{0t} and $\mathbf{u}_{0t'}$ of degenerate branches along this direction radically changes into the point with the index $n_u = -1/2$. And the induction vector fields \mathbf{D}_t and $\mathbf{D}_{t'}$ of the same branches transform the singular pattern of the index $n_D = -2$ into that with the index $n_D = -1/2$. The requirement of the conservation of the topological charge (Poincaré index) is realized in the appearance of three additional conical acoustic axes with indices $n_u = 1/2$ (Alshits, Sarychev & Shuvalov, 1985) and $n_D = -1/2$ (Fig. 11a, b).

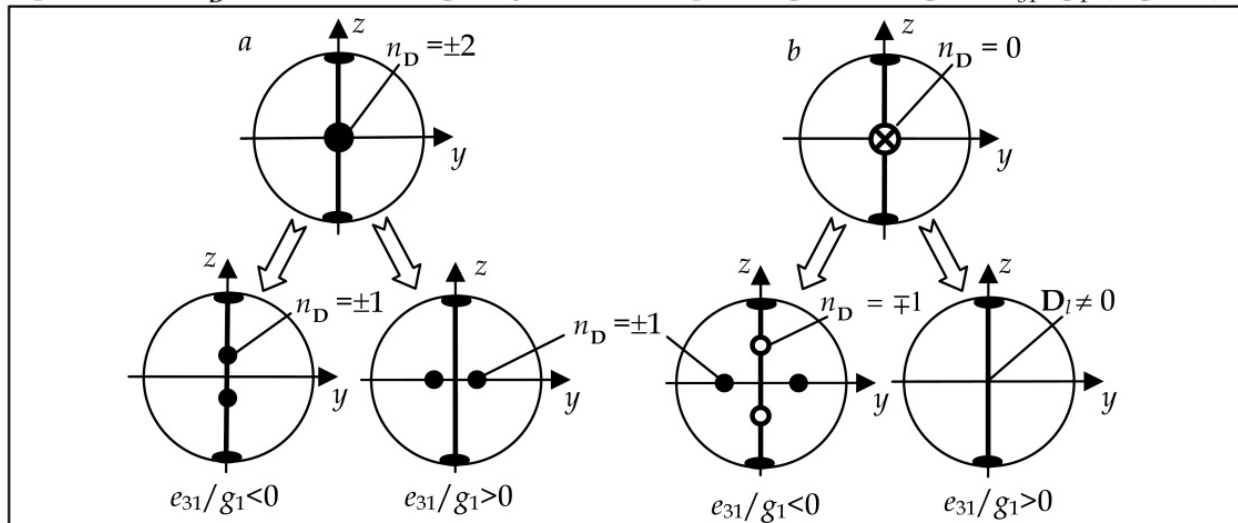


Figure 10. Diagrams illustrating the splitting of singular points with $n_D = \pm 2$ (a) and $n_D = 0$ (b) in a model crystal of the symmetry class $mm2$.

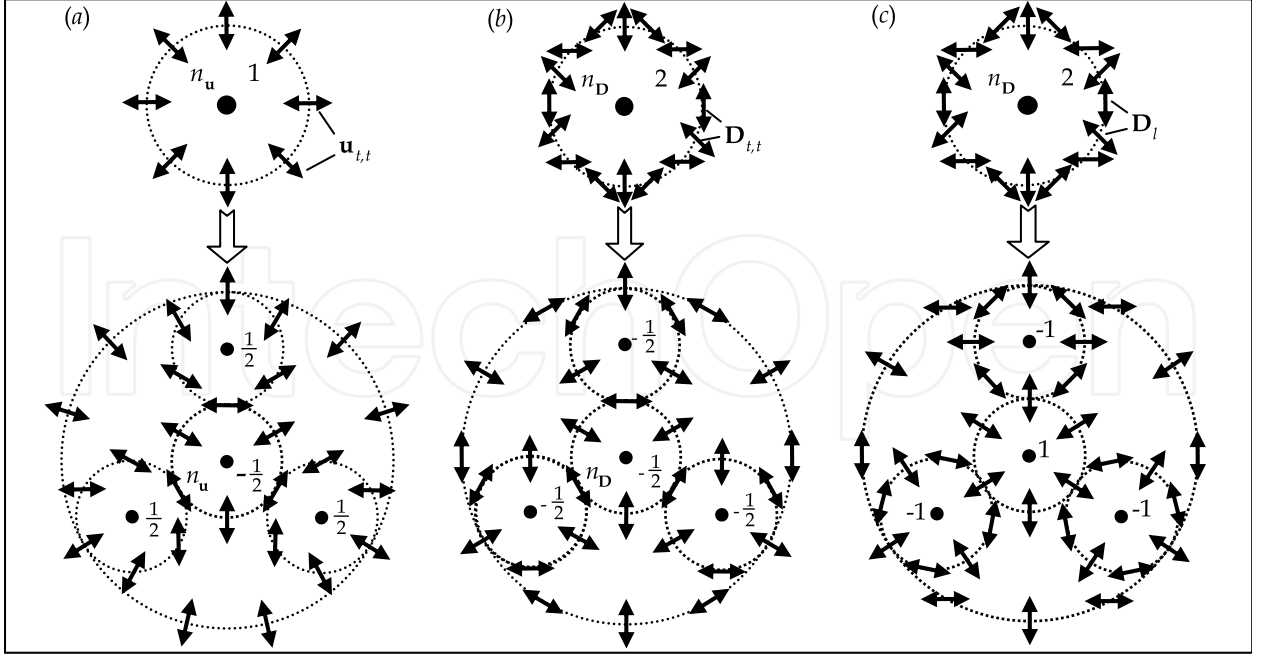


Figure 11. The three topological transformations in the vector fields $\mathbf{u}_{0t,t'}(\mathbf{m})$, $\mathbf{D}_{t,t'}(\mathbf{m})$ and $\mathbf{D}_l(\mathbf{m})$ (in the non-directed representation) after the phase transition $\bar{6} \rightarrow 3$.

In the nondegenerate quasi-longitudinal branch the index $n_D = -2$ is replaced after the transition by $n_D = 1$. In accordance with the same conservation law of the Poincaré index and with the final crystal symmetry, three additional zero-induction points $\mathbf{D}_l = 0$ with the indices $n_D = -1$ must be created along with the central zero-point (Fig. 11c). Thus the considered phase transition ($\bar{6} \rightarrow 3$) causes the three different topological transformations in the vector fields $\mathbf{u}_{0t,t'}(\mathbf{m})$, $\mathbf{D}_{t,t'}(\mathbf{m})$ and $\mathbf{D}_l(\mathbf{m})$ near the principal symmetry axis (Fig.11).

7. Conclusions

Two electric components, the electric field \mathbf{E} and the electric induction \mathbf{D} , accompanying a bulk acoustic wave which propagates in a piezoelectric medium, exhibit significantly different properties. The electric field is always purely longitudinal, whereas the electric induction vector is, in contrast, always purely transverse. On the unit sphere ($\mathbf{m}^2 = 1$) of wave propagation directions, the directions of zero electric field ($\mathbf{E} = 0$) form lines, while the zero-induction directions ($\mathbf{D} = 0$) are usually isolated and appear as singular points of the tangential vector field $\mathbf{D}(\mathbf{m})$ orientations. The nonpiezoactive directions of both types exist practically in all (even triclinic) crystals, although the presence of crystal symmetry elements is the additional factor determining the appearance of such directions.

The topological singularities of the $\mathbf{D}_a(\mathbf{m})$ vector fields in the vicinity of zero-induction points in most crystals are characterized by the Poincaré indices $n_D = \pm 1$, where the sign coincides with that of the determinant of the matrix (62) [see also Eq. (68)]. However, in

some specific cases, this tensor may vanish ($\hat{Q}_a = 0$) in some special directions because of a high symmetry or as a result of vanishing of certain combinations of the material tensor components. In this case, the system has either an isolated zero-induction point \mathbf{m}_0 (and has the Poincaré indices $n_D = 0, \pm 2$) or a zero-induction line. Such special orientations are topologically unstable and, in response to any change in the anisotropy, either split into stable points with $n_D = \pm 1$ or disappear.

It is interesting to note that singularities of the induction vector field $\mathbf{D}_a(\mathbf{m})$ in the vicinity of the zero-induction points substantially differ from analogous singularities near the acoustic axes (see Eq. (71) and Table 3). According to (Alshits *et al*, 1987), stable singularities in the latter case are characterized by the Poincaré indices $n_D = \pm 1/2$, while the unstable ones have $n_D = 0, \pm 1$. The only exception to this rule is the acoustic axis along the hexad axis $\bar{6}$, for which the all branches, both degenerate $a = t, t'$ and non-degenerate $a = l$, are characterized by $\hat{Q}_a = 0$, $\mathbf{D}_a = 0$ and $n_D = -2$. However, as we have seen, in the latter case the transformation of the same singularity $n_D = -2$ due to the phase transition $\bar{6} \rightarrow 3$ has radically different topology [see Fig. 11 (b) and (c)].

Author details

V.I. Alshits

*A.V. Shubnikov Institute of Crystallography, Russian Academy of Sciences, Moscow, Russia
Polish-Japanese Institute of Information Technology, Warsaw, Poland*

V.N. Lyubimov

A.V. Shubnikov Institute of Crystallography, Russian Academy of Sciences, Moscow, Russia

A. Radowicz

Kielce University of Technology, Kielce, Poland

Acknowledgement

This study was performed within the framework of the Agreement on Cooperation between the Shubnikov Institute of Crystallography (Russia) and the Kielce University of Technology (Poland). V.I.A. and V.N.L. are grateful to the Kielce University of Technology for a hospitality and support.

8. References

- Alshits, V.I. & Lothe, J. (1979). Elastic waves in triclinic crystals I, II, and III. *Kristallografiya*, Vol. 24, No. 4, 6 (Aug., Dec. 1979) 972-993, 1122-1130, ISSN 0023-4761 [*Sov. Phys. Crystallography*, Vol. 24, No. 4, 6 (1979) 387-398, 644-648, ISSN 1063-7745]

- Alshits, V.I. & Lyubimov, V.N. (1990). Acoustic waves with extremal electro- (magneto-) mechanical coupling in piezocrystals. *Kristallografiya*, Vol. 35, No. 6 (Dec. 1990) 1325-1327, ISSN 0023-4761 [*Sov. Phys. Crystallography*, Vol. 35, No. 6 (1990) 780-782, ISSN 1063-7745]
- Alshits, V.I.; Lyubimov, V.N. & Radowicz, A. (2005a). Special features of the electric components of acoustic waves in the vicinity of nonpiezoactive directions in crystals. *Zh. Eksp. Teor. Fiz.*, Vol. 128, No. 1 (Jan. 2005) 125-138, ISSN 0044-4510 [*JETP*, Vol. 101, No. 1 (2005) 107-119, ISSN 1063-7761]
- Alshits, V.I.; Lyubimov, V.N. & Radowicz, A. (2005b). Non-piezoactivity in piezoelectrics: basic properties and topological features. *Arch. Appl. Mech.*, Vol. 74, No. 11-12 (Dec. 2005) 739-745, ISSN 0939-1533
- Alshits, V.I.; Lyubimov, V.N.; Sarychev, A.V. & Shuvalov, A.L. (1987). Topological characteristics of singular points of the electric field accompanying sound propagation in piezoelectrics. *Zh. Eksp. Teor. Fiz.*, Vol. 93, No. 2 (8) (Aug. 1987) 723-732, ISSN 0044-4510 [*Sov. Phys. JETP*, Vol. 66, No. 2 (8) (1987) 408-413, ISSN 1063-7761]
- Alshits, V.I.; Sarychev, A.V. & Shuvalov, A.L. (1985). Classification of degeneracies and analysis of their stability in the theory of elastic waves in crystals. *Zh. Eksp. Teor. Fiz.*, Vol. 89, No. 3(9) (Sept. 1985) 922-938, ISSN 0044-4510 [*Sov. Phys. JETP*, Vol. 62, No. 3 (1985) 531-539, ISSN 1063-7761]
- Alshits, V.I. & Shuvalov, A.L. (1988). On acoustic axes in piezoelectric crystals. *Kristallografiya*, Vol. 33, No. 1 (Jan. 1988) 7-12, ISSN 0023-4761 [*Sov. Phys. Crystallography*, Vol. 33, No. 1 (1988) 1-4, ISSN 1063-7745]
- Balakirev, M.K. & Gilinskii, I.A. (1982). *Waves in Piezoelectric Crystals*, Nauka, ISBN, Novosibirsk [in Russian]
- Fedorov, F.I. (1968). *Theory of Elastic Waves in Crystals*, Plenum Press, ISBN, New York
- Gulyaev, Yu.V. (1998). Review of shear surface acoustic waves in solids. *IEEE Trans. Ultrason. Ferroel. Freq. Control*, Vol. 45, No. 4 (April 1998) 935-938, ISSN 0885-3010
- Holm, P. (1992). Generic elastic media. *Phys. Scr.*, Vol. T44 (1992) 122-127, ISSN 0031-8949
- Landau, L.D. & Lifshitz, E.M. (1984). *Electrodynamics of Continuous Media*, Pergamon Press, ISBN 0080302750, New York
- Lyamov, V.E. (1983). *Polarization Effects and Interaction Anisotropy of Acoustic Waves in Crystals*, Moscow State University, ISBN, Moscow [in Russian]
- Lyubimov, V.N. (1969). Consideration of the piezoelectric effect in the theory of elastic waves for crystals of different symmetries. *Doklady AN SSSR*, Vol. 186, No. 5 (May 1969) 1055-1058, ISSN 0869-5652 [*Sov. Phys. Doklady*, Vol. 14, No. 5 (1969) 567-570, ISSN 1085-1992]
- Royer, D. & Dieulesaint, E. (2000). *Elastic Waves in Solids*. Springer, ISBN 3-540-65932-3, Berlin

Shuvalov, A.L. (1998). Topological features of polarization fields of plane acoustic waves in anisotropic media. *Proc. R. Soc. Lond. A*, Vol. 454, (Nov. 1998) 2911-2947, ISSN 1471-2946

Sirotnin Yu.I. & Shaskolskaya, M.P. (1979). *Fundamentals of Crystal Physics* (in Russian), Nauka, Moscow [(1982) translation into English, Mir, ISBN, Moscow]

IntechOpen

IntechOpen